

Threshold resummation for the production of four top quarks at the LHC

Melissa van Beekveld,^{1,*} Anna Kulesza,^{2,3,†} and Laura Moreno Valero^{2,‡}

¹*Rudolf Peierls Centre for Theoretical Physics, Clarendon Laboratory, Parks Road, University of Oxford, Oxford OX1 3PU, UK*

²*Institute for Theoretical Physics, WWU Münster, D-48149 Münster, Germany*

³*Theoretical Physics Department, CERN, 1211 Geneva 23, Switzerland*

(Dated: December 8, 2022)

We compute the total cross section for $t\bar{t}t\bar{t}$ production at next-to-leading logarithmic (NLL') accuracy. This is the first time resummation is performed for a hadron-collider process with four colored particles in the final state. The calculation is matched to the next-to-leading order strong and electroweak corrections. The NLL' corrections enhance the total production rate by 15%. The size of the theoretical error due to scale variation is reduced by more than a factor of two, bringing the theoretical error significantly below the current experimental uncertainty of the measurement.

The production of four top quarks, $pp \rightarrow t\bar{t}t\bar{t}$, is one of the rarest Standard Model (SM) production processes currently accessible experimentally at the Large Hadron Collider (LHC). Its cross section is known to receive significant contributions in various SM extensions, hence an accurate measurement can set strong constraints on new physics models. Examples of such scenarios include supersymmetric theories, where the $t\bar{t}t\bar{t}$ signal can be enhanced by squark and gluino decays [1, 2], the production of a new heavy (pseudo)scalar boson in association with a $t\bar{t}$ pair [3–5], or pair production of scalar gluons [6–9]. Moreover, the $t\bar{t}t\bar{t}$ production rate is sensitive to the Yukawa coupling of the top quark, making it a useful process to further constrain the nature of Higgs-top quark interactions [10, 11]. When interpreted in the framework of an effective theory, a measurement of the $t\bar{t}t\bar{t}$ production process places strong constraints on the four-fermion operator [12–18].

The ATLAS and CMS experiments have searched for the production of $t\bar{t}t\bar{t}$ at the LHC operating at $\sqrt{s} = 13$ TeV [19–24]. In the latest ATLAS analysis [23] a cross section of $\sigma_{t\bar{t}t\bar{t}} = 24 \pm 4(\text{stat.})_{-4}^{+5}(\text{syst.})$ fb is measured, whereas the recent combined analysis of CMS [24] reports a cross section of $\sigma_{t\bar{t}t\bar{t}} = 17_{-5}^{+5}$ fb. Intriguingly, these obtained central values are above the SM prediction, which is calculated at the next-to-leading order (NLO) accuracy both in the strong (QCD) and electroweak (EW) coupling [25–29], with the ATLAS measurement consistent with the SM result only within 2σ . The NLO calculations carry a theoretical error due to scale variation of around 25%, which is comparable with the size of the individual errors of the latest ATLAS and CMS measurements. It is therefore of crucial importance to improve the precision of the theoretical predictions for the $t\bar{t}t\bar{t}$ production, especially having in mind that the future analysis will involve much larger sets of LHC data and the precision of the measurement will increase substantially.

More than 90% of the full NLO result originates from pure QCD interactions. Currently, the calculation of the

next-to-next-to-leading order (NNLO) QCD corrections remains out of reach. However, it is possible to systematically consider a part of higher-order QCD corrections originating from multiple soft gluon emissions. Given the very large partonic centre-of-mass (CM) energy $\sqrt{\hat{s}}$ needed to produce four top quarks, $\sqrt{\hat{s}} \gtrsim 700$ GeV, the $t\bar{t}t\bar{t}$ production at the LHC very often takes place close to production threshold, with any additional real radiation strongly suppressed. One can therefore expect that a large part of the higher-order corrections is due to soft emission and stems from the threshold region. Correspondingly, computing higher-order corrections of this type offers a promising way to improve the precision of the prediction.

Higher-order QCD corrections from soft gluon emission can be systematically taken into account using resummation, either in direct QCD or in the soft-collinear effective-field-theory framework. The resummation programme for processes involving multiple top quarks has been very successful over the recent years, leading to substantial improvements of theoretical precision for the calculation of the total production cross section for such processes, such as top-pair production [30–39] or $t\bar{t}H/Z/W^\pm/\gamma$ [40–52]. However, in contrast to $t\bar{t}t\bar{t}$, these processes involve at most two coloured particles in the final state. To the best of our knowledge, resummation for processes involving a higher number of coloured particles has not been achieved before.

In this work, we perform for the first time the resummation of a process with 4 coloured particles at the Born level by applying direct QCD resummation methods in Mellin space to the process $pp \rightarrow t\bar{t}t\bar{t}$. The calculations are carried out at the next-to-leading logarithmic (NLL) accuracy, and take into account constant $\mathcal{O}(\alpha_s)$ non-logarithmic contributions that do not vanish at threshold (referred to as NLL' accuracy).

I. METHODOLOGY

Soft-gluon corrections get logarithmically large at the absolute production threshold when $\sqrt{\hat{s}}$ approaches $M \equiv 4m_t$, with m_t the mass of the top quark. This corre-

* melissa.vanbeekveld@physics.ox.ac.uk

† anna.kulesza@uni-muenster.de

‡ l.more02@uni-muenster.de

sponds to the limit $\hat{\rho} \rightarrow 1$ of the partonic threshold variable, $\hat{\rho} \equiv M^2/\hat{s}$. The theory of $2 \rightarrow 4$ threshold resummation builds on the theory resummation for $2 \rightarrow 2$ processes [31, 53–55]. We work in Mellin space, where the hadronic cross section $\sigma_{t\bar{t}\bar{t}\bar{t}}(N)$ is the Mellin transform w.r.t. the variable $\rho \equiv M^2/s$

$$\sigma_{t\bar{t}\bar{t}\bar{t}}(N) = \int_0^1 d\rho \rho^{N-1} \sigma_{t\bar{t}\bar{t}\bar{t}}(\rho) \quad (1)$$

of the hadronic cross section in momentum space

$$\begin{aligned} \sigma_{t\bar{t}\bar{t}\bar{t}}(\rho) = & \sum_{i,j} \int_0^1 dx_1 f_i(x_1, \mu_F^2) \int_0^1 dx_2 f_j(x_2, \mu_F^2) \\ & \times \int_\rho^1 d\hat{\rho} \delta\left(\hat{\rho} - \frac{\rho}{x_1 x_2}\right) \hat{\sigma}_{ij \rightarrow t\bar{t}\bar{t}\bar{t}}(\hat{\rho}). \end{aligned} \quad (2)$$

Here we use f_i to denote parton distribution functions (PDFs), μ_F the factorisation scale, and $x_{1,2}$ the momentum fraction of the two colliding partons i, j . Only two partonic channels contribute at leading order (LO), $ij = \{q\bar{q}, gg\}$. The cross section $\hat{\sigma}_{ij \rightarrow t\bar{t}\bar{t}\bar{t}}(N)$ is a purely perturbative function that obeys a refactorisation in the soft and collinear limits into functions containing information on particular modes of dynamics. Correspondingly, one can identify a soft function \mathbf{S} , containing corrections originating from soft gluon radiation, a collinear / jet function for each initial-state leg Δ_i , containing corrections from collinear gluon radiation. All terms that are non-logarithmic in the soft-gluon limit are collected in the hard function \mathbf{H} . These functions are defined at the cross section level, i.e. they include the necessary phase-space integrals. The factorisation in Mellin space takes the form

$$\begin{aligned} \hat{\sigma}_{ij \rightarrow t\bar{t}\bar{t}\bar{t}}^{\text{res}}(N) = & \Delta_i(N+1) \Delta_j(N+1) \\ & \times \text{Tr} \left[\tilde{\mathbf{S}}_{ij \rightarrow t\bar{t}\bar{t}\bar{t}}(N+1) \otimes \mathbf{H}_{ij \rightarrow t\bar{t}\bar{t}\bar{t}}(N) \right], \end{aligned} \quad (3)$$

suppressing the dependence of the various ingredients on the factorisation and renormalisation scales. As the jet and soft functions both capture soft-collinear enhancements, care must be taken to subtract the overlap contributions. In practice, this is done by dividing out the eikonal jet functions \mathcal{J}_i from the soft function. This results in a new soft-collinear subtracted soft function that is denoted by $\tilde{\mathbf{S}}$, and related to the full soft function as

$$\tilde{\mathbf{S}}(N+1) = \frac{\mathbf{S}(N+1)}{\mathcal{J}_1(N+1) \mathcal{J}_2(N+1)}. \quad (4)$$

The soft and hard functions are generally matrices in colour space, as indicated by their bold font, and colour-connected, indicated by the \otimes -symbol. We now briefly go over the definition for each of the ingredients in Eq. (3).

The hard function $\mathbf{H}_{ij \rightarrow t\bar{t}\bar{t}\bar{t}}$ in Eq. (3) obeys the perturbative expansion

$$\mathbf{H}_{ij \rightarrow t\bar{t}\bar{t}\bar{t}} = \mathbf{H}_{ij \rightarrow t\bar{t}\bar{t}\bar{t}}^{(0)} + \frac{\alpha_s}{\pi} \mathbf{H}_{ij \rightarrow t\bar{t}\bar{t}\bar{t}}^{(1)} + \mathcal{O}(\alpha_s^2). \quad (5)$$

At the NLL accuracy we need $\mathbf{H}_{ij \rightarrow t\bar{t}\bar{t}\bar{t}}^{(0)}$, defined as a matrix in colour space with an element IJ

$$\mathbf{H}_{ij \rightarrow t\bar{t}\bar{t}\bar{t}, IJ}^{(0)} = \frac{1}{2\hat{s}} \int_0^1 d\hat{\rho} \hat{\rho}^{N-1} \int d\Phi^B \sum_{\text{colour, spin}} \mathcal{A}_I^{(0)} \mathcal{A}_J^{\dagger(0)}, \quad (6)$$

where we sum (average) over final(initial)-state colour and polarization degrees of freedom. The Born phase space is denoted by Φ^B . The object $\mathcal{A}_I^{(0)} = \langle c_I | \mathcal{A}^{(0)} \rangle$ is the colour-stripped amplitude projected to the colour-vector c_I , with $|\mathcal{A}^{(0)}\rangle$ the amplitude in the corresponding colour basis, while $\mathcal{A}_J^{(0)\dagger}$ is its complex conjugate projected to c_J^\dagger . We obtain the squared matrix elements numerically from aMC@NLO [26, 56], after selecting a suitable colour basis as discussed below.

The coefficient $\mathbf{H}_{ij \rightarrow t\bar{t}\bar{t}\bar{t}}^{(1)}$ enters formally at next-to-next-to-leading logarithmic accuracy but can be used to supplement the NLL expressions, resulting in NLL' precision. It consists of virtual one-loop corrections, $\mathbf{V}_{ij \rightarrow t\bar{t}\bar{t}\bar{t}}^{(1)}$, and constant terms stemming from collinear-enhanced contributions $\mathbf{C}_{ij \rightarrow t\bar{t}\bar{t}\bar{t}}^{(1)}$ that are not yet captured by the initial-state jet functions Δ_i , i.e.

$$\mathbf{H}_{ij \rightarrow t\bar{t}\bar{t}\bar{t}}^{(1)} = \mathbf{V}_{ij \rightarrow t\bar{t}\bar{t}\bar{t}}^{(1)} + \mathbf{C}_{ij \rightarrow t\bar{t}\bar{t}\bar{t}}^{(1)}. \quad (7)$$

While the $\mathbf{C}_{ij \rightarrow t\bar{t}\bar{t}\bar{t}}^{(1)}$ coefficient is calculated analytically, the $\mathbf{V}_{ij \rightarrow t\bar{t}\bar{t}\bar{t}}^{(1)}$ coefficient is obtained numerically using MadLoop [57–60]. We have explicitly checked that the infrared pole structure of the MadLoop calculation, using FKS subtraction [61–63], matches that of our resummed calculation.

For the incoming jet functions we use the well-known expressions that can be found in e.g. [64–66], which are a function of $\lambda = \alpha_s b_0 \ln \bar{N}$ with $\bar{N} \equiv N e^{\gamma_E}$. The soft function is given by [31, 53]

$$\mathbf{S}_{ij \rightarrow t\bar{t}\bar{t}\bar{t}} = \bar{\mathbf{U}}_{ij \rightarrow t\bar{t}\bar{t}\bar{t}} \tilde{\mathbf{S}}_{ij \rightarrow t\bar{t}\bar{t}\bar{t}} \mathbf{U}_{ij \rightarrow t\bar{t}\bar{t}\bar{t}}, \quad (8)$$

with the evolution matrix written as a path-ordered exponential

$$\mathbf{U}_{ij \rightarrow t\bar{t}\bar{t}\bar{t}} = P \exp \left[\frac{1}{2} \int_{\mu_r^2}^{M^2/\bar{N}^2} \frac{dq^2}{q^2} \mathbf{\Gamma}_{ij \rightarrow t\bar{t}\bar{t}\bar{t}}(\alpha_s(q^2)) \right], \quad (9)$$

and $\mathbf{\Gamma}_{ij \rightarrow t\bar{t}\bar{t}\bar{t}}(\alpha_s(q^2))$ the soft anomalous dimension matrix. To achieve NLL' resummation we need to know the one-loop contribution $\mathbf{\Gamma}_{ij \rightarrow t\bar{t}\bar{t}\bar{t}}^{(1)}$ in Eq. (9). This object consists of a kinematic part and a colour-mixing part, which accounts for the change in colour of the hard system, i.e.

$$\mathbf{\Gamma}_{ij \rightarrow t\bar{t}\bar{t}\bar{t}, IJ}^{(1)} = \sum_{k,l=1}^6 \text{Tr} \left[c_I \mathbf{T}_k \cdot \mathbf{T}_l c_J^\dagger \right] \Gamma_{kl}, \quad (10)$$

where \mathbf{T}_k are colour operators. The explicit expression for $\mathbf{\Gamma}_{ij \rightarrow t\bar{t}\bar{t},IJ}^{(1)}$ depends on a choice of basis tensors represented by c_I (and c_J^\dagger for the complex conjugate) for the underlying hard scattering process $ij \rightarrow t\bar{t}\bar{t}$. The kinematic part, Γ_{kl} , is given by the residue of the UV-divergent part of the one-loop eikonal contributions [30, 67, 68].

The matrix $\tilde{\mathbf{S}}_{ij \rightarrow t\bar{t}\bar{t}}$ in Eq. (8) represents the boundary condition for the solution of the renormalisation group equation at $\mu_R = M/\bar{N}$ from which Eq. (8) follows. Like \mathbf{H} , it obeys a perturbative expansion which reads

$$\tilde{\mathbf{S}}_{ij \rightarrow t\bar{t}\bar{t}} = \tilde{\mathbf{S}}_{ij \rightarrow t\bar{t}\bar{t}}^{(0)} + \frac{\alpha_s}{\pi} \tilde{\mathbf{S}}_{ij \rightarrow t\bar{t}\bar{t}}^{(1)} + \mathcal{O}(\alpha_s^2). \quad (11)$$

The lowest-order contribution $\tilde{\mathbf{S}}_{ij \rightarrow t\bar{t}\bar{t}}^{(0)}$ is given by the trace of the colour basis vectors for the underlying hard process. For NLL' resummation we also need the first-order correction $\tilde{\mathbf{S}}_{ij \rightarrow t\bar{t}\bar{t}}^{(1)}$, which is calculated analytically by considering the eikonal corrections to $\tilde{\mathbf{S}}_{ij \rightarrow t\bar{t}\bar{t}}^{(0)}$.

The major difficulty in the resummed calculations for the $t\bar{t}\bar{t}$ production cross section stems from the complicated colour structure of the underlying hard process, involving six coloured particles. The colour structure of the $q\bar{q} \rightarrow t\bar{t}\bar{t}$ process is

$$\mathbf{3} \otimes \bar{\mathbf{3}} = \mathbf{3} \otimes \bar{\mathbf{3}} \otimes \mathbf{3} \otimes \bar{\mathbf{3}}. \quad (12)$$

The decomposition into irreducible representations reads

$$\mathbf{1} \oplus \mathbf{8} = (2 \times \mathbf{1}) \oplus (2 \times \mathbf{8}) \oplus \mathbf{8}_S \oplus \mathbf{8}_A \oplus \mathbf{10} \oplus \bar{\mathbf{10}} \oplus \mathbf{27}. \quad (13)$$

For the gg channel we have

$$\mathbf{8} \otimes \mathbf{8} = \mathbf{3} \otimes \bar{\mathbf{3}} \otimes \mathbf{3} \otimes \bar{\mathbf{3}}, \quad (14)$$

and in terms of irreducible representations

$$\begin{aligned} \mathbf{0} \oplus \mathbf{1} \oplus \mathbf{8}_S \oplus \mathbf{8}_A \oplus \mathbf{10} \oplus \bar{\mathbf{10}} \oplus \mathbf{27} = \\ \mathbf{0} \oplus (2 \times \mathbf{1}) \oplus (2 \times \mathbf{8}) \oplus \mathbf{8}_S \oplus \mathbf{8}_A \oplus \mathbf{10} \oplus \bar{\mathbf{10}} \oplus \mathbf{27}. \end{aligned} \quad (15)$$

From this we infer that the $q\bar{q}$ colour space is 6-dimensional, whereas the gg one is 14-dimensional, directly translating into the dimensions of the soft anomalous dimension matrices of Eq. (10).

Moreover, the one-loop soft anomalous dimension matrices $\mathbf{\Gamma}_{ij \rightarrow t\bar{t}\bar{t}}^{(1)}$ are in general not diagonal. Solving Eq. (9) in terms of standard exponential functions requires changing the colour bases to R where $\mathbf{\Gamma}_{ij \rightarrow t\bar{t}\bar{t},R}^{(1)}$ is diagonal [53]. We find such orthonormal bases using the technique outlined in Ref. [69]. The resulting one-loop soft anomalous dimension matrices for $N_c = 3$ in the threshold limit become ¹

$$2\text{Re}[\bar{\mathbf{\Gamma}}_{q\bar{q} \rightarrow t\bar{t}\bar{t},R}] = \text{diag}(0, 0, -3, -3, -3, -3), \quad (16a)$$

$$2\text{Re}[\bar{\mathbf{\Gamma}}_{gg \rightarrow t\bar{t}\bar{t},R}] = \text{diag}(-8, -6, -6, -4, -3, -3, -3, -3, -3, -3, 0, 0). \quad (16b)$$

The values above are the negative values of the quadratic Casimir invariants for the irreducible representations in which the colour structure of the final state can be decomposed in SU(3). This result corresponds to a physical picture where the soft gluon is only sensitive to the total colour charge of a system at threshold, and constitutes a strong check of our calculations. We have also verified that the virtual corrections obtained from MadLoop, rewritten in the new basis R , are consistently 0 for the base vector corresponding to a representation whose dimension is zero for $N_c = 3$, which is another important consistency check of our work.

With this, the contribution of the soft-collinear-subtracted soft function in Mellin space reads

$$\begin{aligned} \tilde{\mathbf{S}}_{ij \rightarrow t\bar{t}\bar{t},R}(N) = \\ \tilde{\mathbf{S}}_{ij \rightarrow t\bar{t}\bar{t},R} \exp \left[\frac{\text{Re}[\bar{\mathbf{\Gamma}}_{ij \rightarrow t\bar{t}\bar{t},R}^{(1)}]}{b_0 \pi} \ln(1 - 2\lambda) \right], \end{aligned} \quad (17)$$

where $\bar{\mathbf{\Gamma}}_{ij \rightarrow t\bar{t}\bar{t},R}^{(1)}$ is related to $\mathbf{\Gamma}_{ij \rightarrow t\bar{t}\bar{t},R}^{(1)}$ after subtracting the soft-collinear contributions [54]. Note that the hard function in Eq. (3) also needs to be written in terms of the colour tensor basis R , requiring us to transform from the trace-basis used in aMC@NLO to our new basis.

The last step to calculate a physical cross section in momentum space involves taking the inverse Mellin transform of the N -space expression

$$\begin{aligned} \sigma_{t\bar{t}\bar{t}}^{\text{f.o.}+\text{res}}(\rho) = \sigma_{t\bar{t}\bar{t}}^{\text{f.o.}}(\rho) + \\ \sum_{ij} \int_{\mathcal{C}} \frac{dN}{2\pi i} \rho^{-N} f_i(N+1, \mu_F^2) f_j(N+1, \mu_F^2) \\ \times \left[\hat{\sigma}_{ij \rightarrow t\bar{t}\bar{t}}^{\text{res}}(N) - \hat{\sigma}_{ij \rightarrow t\bar{t}\bar{t}}^{\text{res}}(N) \Big|_{\mathcal{O}(\alpha_s^n)} \right], \end{aligned} \quad (18)$$

where ‘res’ denotes LL, NLL or NLL'. To retain the full available information from the perturbative calculation, we match the resummed result to the fixed-order cross section $\sigma^{\text{f.o.}}$, leading to the ‘f.o. +res’ accuracy. To avoid double-counting, the resummed result is expanded up to $\mathcal{O}(\alpha_s^n)$ (denoted as $\hat{\sigma}_{ij \rightarrow t\bar{t}\bar{t}}^{\text{res}}(N) \Big|_{\mathcal{O}(\alpha_s^n)}$), with $n = 4$ for f.o.=LO or $n = 5$ for f.o.=NLO. The inverse Mellin transform in Eq. (18) relies on the so-called Minimal Prescription [71] and is evaluated numerically on a contour \mathcal{C} parameterised by C_{MP} and ϕ_{MP} as

$$N = C_{\text{MP}} + ye^{i\phi_{\text{MP}}}, \quad (19)$$

with $y \in [0, \infty)$. We calculated results for various values C_{MP} and ϕ_{MP} to verify the independence of the result on the choice of the contour.

¹ Their full forms will be given in Ref. [70].

II. NUMERICAL RESULTS

The phenomenological studies reported in this letter are performed using the central member of the LUXqed_plus_PDF4LHC15_nnlo_100 PDF set [72, 73] for both the pure QCD results and the QCD + EW results. This PDF set is based on the PDF4LHC15 PDF set [74–77] and includes the photon content of the proton, needed for the calculation of the EW corrections. We use the α_s value corresponding to the PDF set, take the mass of the top quark $m_t = 172.5$ GeV (unless stated otherwise) and choose the central factorisation and renormalisation scale $\mu_{F,0} = \mu_{R,0} = 2m_t$. The theoretical uncertainty is estimated by varying μ_R and μ_F using a 7-point scale variation. To this end, we consider the minimal and maximum cross section values calculated for

$$\left(\frac{\mu_R}{\mu_{R,0}}, \frac{\mu_F}{\mu_{F,0}} \right)_{7\text{-point}} \in \{(0.5, 0.5), (0.5, 1), (1, 0.5), (1, 1), (1, 2), (2, 1), (2, 2)\}. \quad (20)$$

The fixed-order results are obtained using aMC@NLO [26, 56]. Since our calculation concerns pure QCD corrections, we present the LO and NLO QCD results for comparison. However, our final resummation-improved cross section incorporates the NLO(QCD+EW) result, where the electroweak corrections are included up to $\mathcal{O}(\alpha^2)$ [28].² We show our results for \bar{N} resummation, but did confirm that those for N -resummation show qualitatively the same behaviour. We defer a detailed discussion of the subtle differences between N and \bar{N} resummation to an upcoming publication [70].

In Fig. 1 we show the scale dependence of various fixed-order and matched resummed results for $\sigma_{t\bar{t}t\bar{t}}$ under the assumption $\mu_R = \mu_F$. While the NLL corrections only moderately improve the scale dependence of the NLO QCD cross section, the scale sensitivity of the NLO+NLL' result is dramatically reduced. NLL' contributions increase the $\sigma_{t\bar{t}t\bar{t}}$ predictions by 16% w.r.t. the pure NLO QCD result, and by 15% w.r.t. the complete NLO (QCD+EW) result, see the reported $K_{\text{NLL}'}$ factors in Table I. These corrections are more than twice the size of the previously calculated complete EW effects at NLO.

Next we examine the reduction of the theoretical error of the resummation-improved cross section using the 7-point method. In Table I we quote the central values of the NLO, NLO(QCD+EW), NLO+NLL' and NLO(QCD+EW)+NLL' cross sections together with the corresponding error due to scale variation. This information is graphically represented in Fig. 2. We see that the 7-point method scale error gets smaller with increasing accuracy of the calculations. Remarkably, the scale error of the NLO+NLL' predictions is reduced compared to NLO predictions by more than a factor of 2. Including the PDF uncertainty of $\pm 6.9\%$, our state-of-the-art

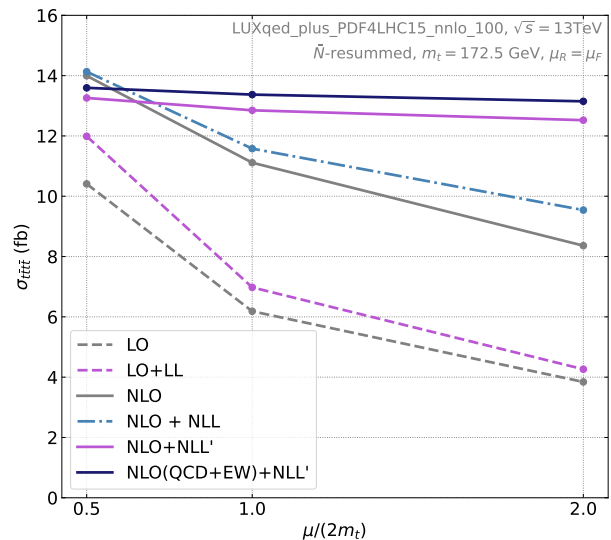


FIG. 1. Scale dependence of the pure QCD LO (gray dashed), NLO (gray solid), LO+LL (purple dashed), NLO+NLL (light-blue dash-dotted), NLO+NLL' (blue solid) and NLO(QCD+EW)+NLL' (dark-blue solid) cross sections at $\sqrt{s} = 13$ TeV, obtained by varying $\mu = \mu_R = \mu_F$ with a factor of 2 around the central scale of $\mu_0 = 2m_t$.

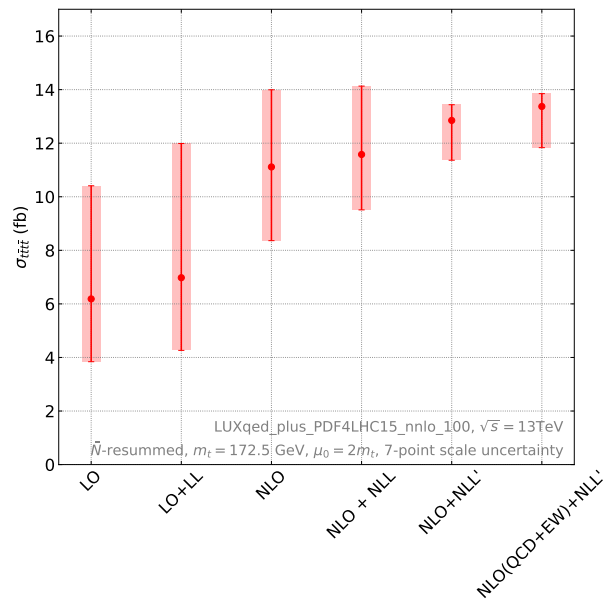


FIG. 2. Predictions for the total $pp \rightarrow t\bar{t}t\bar{t}$ cross section at $\sqrt{s} = 13$ TeV for fixed-order calculations and resummation-improved results, obtained using the 7-point scale variation as indicated in Eq. (20).

predictions for $\sqrt{s} = 13$ TeV and $m_t = 172.5$ GeV read

$$\sigma_{t\bar{t}t\bar{t}}^{\text{NLO(QCD+EW)+NLL}'} = 13.37(2)_{-1.52}^{+0.48}(\text{scale}) \pm 0.92(\text{pdf}) \text{ fb},$$

or, adding the two theoretical errors in quadrature

$$\sigma_{t\bar{t}t\bar{t}}^{\text{NLO(QCD+EW)+NLL}'} = 13.37(2)_{-1.78}^{+1.04} \text{ fb}. \quad (21)$$

² In the notation of Ref. [28], we include up to (N)LO₃.

\sqrt{s} (TeV)	$\sigma_{t\bar{t}t\bar{t}}^{\text{NLO}}$ (fb)	$\sigma_{t\bar{t}t\bar{t}}^{\text{NLO+NLL}}$ (fb)	$\sigma_{t\bar{t}t\bar{t}}^{\text{NLO+NLL}'}$ (fb)	$K_{\text{NLL}'}$
13	11.00(2) $^{+25.2\%}_{-24.5\%}$ fb	11.46(2) $^{+21.3\%}_{-17.7\%}$ fb	12.73(2) $^{+4.1\%}_{-11.8\%}$ fb	1.16
13.6	13.14(2) $^{+25.1\%}_{-24.4\%}$ fb	13.81(2) $^{+20.7\%}_{-20.1\%}$ fb	15.16(2) $^{+2.5\%}_{-11.9\%}$ fb	1.15
\sqrt{s} (TeV)	$\sigma_{t\bar{t}t\bar{t}}^{\text{NLO(QCD+EW)}}$ (fb)	$\sigma_{t\bar{t}t\bar{t}}^{\text{NLO(QCD+EW)+NLL}}$ (fb)	$\sigma_{t\bar{t}t\bar{t}}^{\text{NLO(QCD+EW)+NLL}'}$ (fb)	$K_{\text{NLL}'}$
13	11.64(2) $^{+23.2\%}_{-22.8\%}$ fb	12.10(2) $^{+19.5\%}_{-16.3\%}$ fb	13.37(2) $^{+3.6\%}_{-11.4\%}$ fb	1.15
13.6	13.80(2) $^{+22.6\%}_{-22.9\%}$ fb	14.47(2) $^{+18.5\%}_{-19.1\%}$ fb	15.82(2) $^{+1.5\%}_{-11.6\%}$ fb	1.15

TABLE I. Fixed and resummed-and-matched total cross sections in fb for $pp \rightarrow t\bar{t}t\bar{t}$ with $\sqrt{s} = 13$ TeV and $\sqrt{s} = 13.6$ TeV, the central scale value of $\mu_0 = 2m_t$ and $m_t = 172.5$ GeV. The number in parenthesis indicates the statistical uncertainty on the last digit whereas the percentage error indicates the 7-point scale uncertainty, obtained using the variations indicated in Eq. (20). The $K_{\text{NLL}'}$ factor is the ratio of the resummation-improved cross section at NLO+NLL' to the NLO cross section.

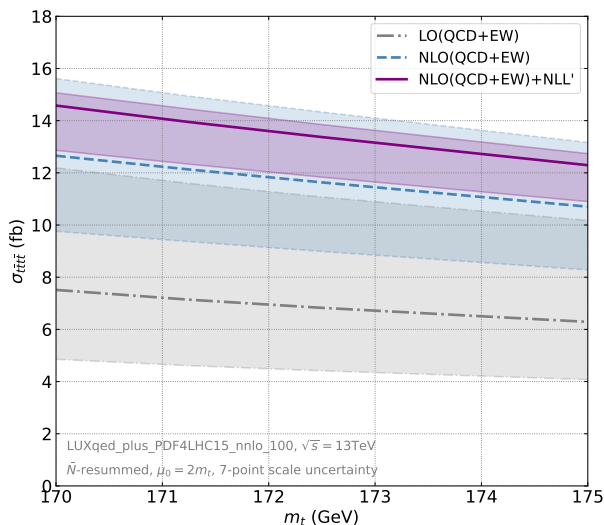


FIG. 3. Cross section for the $pp \rightarrow t\bar{t}t\bar{t}$ process with $\sqrt{s} = 13$ TeV for different values of m_t . Shown are the LO, NLO and NLO+NLL' predictions (QCD + EW). The bands indicates the scale uncertainty calculated using the 7-point method, where the central scale is taken to be $\mu_0 = 2m_t$.

In Table I we also report the obtained cross section for the LHC CM energy of 13.6 TeV. Including the scale uncertainty of $\pm 6.7\%$ we obtain

$$\begin{aligned} \sigma_{t\bar{t}t\bar{t}}^{\text{NLO(QCD+EW)+NLL}'} &= 15.82(2)_{-1.83}^{+0.24}(\text{scale}) \pm 1.06(\text{pdf}) \text{ fb} \\ &= 15.82(2)_{-2.11}^{+1.09} \text{ fb}, \end{aligned}$$

which is an increase of 18.3% w.r.t. the obtained cross section for $\sqrt{s} = 13$ TeV.

We have also studied the effect of varying the value of the top mass in the window of $[170 - 175]$ GeV. The resulting predictions are shown in Fig. 3 for $\sqrt{s} = 13$ TeV. We observe that the correction stemming from soft-gluon resummation is flat under variation of the top quark mass.

III. CONCLUSION

In this letter, we have obtained predictions for the total cross section of the four top production process at NLO+NLL' accuracy, including electroweak corrections for the fixed-order prediction. This is the first time that the framework of threshold resummation has been applied to a $2 \rightarrow 4$ process containing six coloured partons at leading order. We present our results both at a collider energy of 13 and 13.6 TeV, and vary the top mass in the window of 170–175 GeV. Setting $m_t = 172.5$ GeV and $\sqrt{s} = 13.6$ TeV, we find the total cross section $\sigma_{t\bar{t}t\bar{t}}^{\text{NLO(QCD+EW)+NLL}'} = 15.8_{-11.6\%}^{+1.5\%}$ fb, where the indicated error is estimated using the 7-point scale uncertainty. When compared to the NLO(QCD+EW)-only prediction, $\sigma_{t\bar{t}t\bar{t}}^{\text{NLO(QCD+EW)}} = 13.8_{-22.9\%}^{+22.6\%}$ fb, we find that the central value is increased with a K -factor of 1.15. The uncertainty stemming from scale variation is reduced by more than a factor of two. Including the PDF error in quadrature we reduce the total theoretical uncertainty from $(+23.6\%, -23.9\%)$ at NLO(QCD+EW) to $(+6.8\%, -13.4\%)$ at NLO(QCD + EW)+NLL', which lies comfortably below the current experimental uncertainty. These predictions will play an important role in stress-testing the SM, especially in view of the latest experimental results obtained for $t\bar{t}t\bar{t}$ production.

ACKNOWLEDGEMENTS

We are grateful to Marco Zaro and Davide Pagani for their help in extracting the NLO electroweak corrections from aMC@NLO. This work has been supported in part by the DFG grant KU 3103/2. MvB acknowledges support from a Royal Society Research Professorship (RP/R1/180112) and from the Science and Technology Facilities Council under grant ST/T000864/1, while LMV acknowledges support from the DFG Research Training Group “GRK 2149: Strong and Weak Interactions - from Hadrons to Dark Matter”. AK gratefully acknowledges the support and the hospitality of the

-
- [1] G. R. Farrar and P. Fayet, Phenomenology of the production, decay, and detection of new hadronic states associated with supersymmetry, *Physics Letters B* **76**, 575 (1978).
- [2] M. Toharia and J. D. Wells, Gluino decays with heavier scalar superpartners, *JHEP* **02**, 015, arXiv:hep-ph/0503175.
- [3] D. Dicus, A. Stange, and S. Willenbrock, Higgs decay to top quarks at hadron colliders, *Phys. Lett. B* **333**, 126 (1994), arXiv:hep-ph/9404359.
- [4] N. Craig, F. D’Eramo, P. Draper, S. Thomas, and H. Zhang, The Hunt for the Rest of the Higgs Bosons, *JHEP* **06**, 137, arXiv:1504.04630 [hep-ph].
- [5] N. Craig, J. Hajer, Y.-Y. Li, T. Liu, and H. Zhang, Heavy Higgs bosons at low $\tan\beta$: from the LHC to 100 TeV, *JHEP* **01**, 018, arXiv:1605.08744 [hep-ph].
- [6] T. Plehn and T. M. P. Tait, Seeking Sgluons, *J. Phys. G* **36**, 075001 (2009), arXiv:0810.3919 [hep-ph].
- [7] S. Calvet, B. Fuks, P. Gris, and L. Valery, Searching for sgluons in multitop events at a center-of-mass energy of 8 TeV, *JHEP* **04**, 043, arXiv:1212.3360 [hep-ph].
- [8] L. Beck, F. Blekman, D. Dobur, B. Fuks, J. Keaveney, and K. Mawatari, Probing top-philic sgluons with LHC Run I data, *Phys. Lett. B* **746**, 48 (2015), arXiv:1501.07580 [hep-ph].
- [9] L. Darmé, B. Fuks, and M. Goodsell, Cornering sgluons with four-top-quark events, *Phys. Lett. B* **784**, 223 (2018), arXiv:1805.10835 [hep-ph].
- [10] Q.-H. Cao, S.-L. Chen, and Y. Liu, Probing Higgs Width and Top Quark Yukawa Coupling from $t\bar{t}H$ and $t\bar{t}t\bar{t}$ Productions, *Phys. Rev. D* **95**, 053004 (2017), arXiv:1602.01934 [hep-ph].
- [11] Q.-H. Cao, S.-L. Chen, Y. Liu, R. Zhang, and Y. Zhang, Limiting top quark-Higgs boson interaction and Higgs-boson width from multitop productions, *Phys. Rev. D* **99**, 113003 (2019), arXiv:1901.04567 [hep-ph].
- [12] C. Zhang, Constraining $q\bar{q}t\bar{t}$ operators from four-top production: a case for enhanced EFT sensitivity, *Chin. Phys. C* **42**, 023104 (2018), arXiv:1708.05928 [hep-ph].
- [13] G. Banelli, E. Salvioni, J. Serra, T. Theil, and A. Weiler, The Present and Future of Four Top Operators, *JHEP* **02**, 043, arXiv:2010.05915 [hep-ph].
- [14] D. Barducci *et al.*, Interpreting top-quark LHC measurements in the standard-model effective field theory, (2018), arXiv:1802.07237 [hep-ph].
- [15] N. P. Hartland, F. Maltoni, E. R. Nocera, J. Rojo, E. Slade, E. Vryonidou, and C. Zhang, A Monte Carlo global analysis of the Standard Model Effective Field Theory: the top quark sector, *JHEP* **04**, 100, arXiv:1901.05965 [hep-ph].
- [16] J. J. Ethier, G. Magni, F. Maltoni, L. Mantani, E. R. Nocera, J. Rojo, E. Slade, E. Vryonidou, and C. Zhang (SMEFiT), Combined SMEFT interpretation of Higgs, diboson, and top quark data from the LHC, *JHEP* **11**, 089, arXiv:2105.00006 [hep-ph].
- [17] L. Darmé, B. Fuks, and F. Maltoni, Top-philic heavy resonances in four-top final states and their EFT interpretation, *JHEP* **09**, 143, arXiv:2104.09512 [hep-ph].
- [18] R. Aoude, H. El Faham, F. Maltoni, and E. Vryonidou, Complete SMEFT predictions for four top quark production at hadron colliders, *JHEP* **10**, 163, arXiv:2208.04962 [hep-ph].
- [19] A. M. Sirunyan *et al.* (CMS), Search for production of four top quarks in final states with same-sign or multiple leptons in proton-proton collisions at $\sqrt{s} = 13$ TeV, *Eur. Phys. J. C* **80**, 75 (2020), arXiv:1908.06463 [hep-ex].
- [20] A. M. Sirunyan *et al.* (CMS), Search for the production of four top quarks in the single-lepton and opposite-sign dilepton final states in proton-proton collisions at $\sqrt{s} = 13$ TeV, *JHEP* **11**, 082, arXiv:1906.02805 [hep-ex].
- [21] M. Aaboud *et al.* (ATLAS), Search for four-top-quark production in the single-lepton and opposite-sign dilepton final states in pp collisions at $\sqrt{s} = 13$ TeV with the ATLAS detector, *Phys. Rev. D* **99**, 052009 (2019), arXiv:1811.02305 [hep-ex].
- [22] G. Aad *et al.* (ATLAS), Evidence for $t\bar{t}t\bar{t}$ production in the multilepton final state in proton-proton collisions at $\sqrt{s} = 13$ TeV with the ATLAS detector, *Eur. Phys. J. C* **80**, 1085 (2020), arXiv:2007.14858 [hep-ex].
- [23] G. Aad *et al.* (ATLAS), Measurement of the $t\bar{t}t\bar{t}$ production cross section in pp collisions at $\sqrt{s} = 13$ TeV with the ATLAS detector, *JHEP* **11**, 118, arXiv:2106.11683 [hep-ex].
- [24] *Evidence for the simultaneous production of four top quarks in proton-proton collisions at $\sqrt{s} = 13$ TeV*, Tech. Rep. (CERN, Geneva, 2022).
- [25] G. Bevilacqua and M. Worek, Constraining BSM Physics at the LHC: Four top final states with NLO accuracy in perturbative QCD, *JHEP* **07**, 111, arXiv:1206.3064 [hep-ph].
- [26] J. Alwall, R. Frederix, S. Frixione, V. Hirschi, F. Maltoni, O. Mattelaer, H. S. Shao, T. Stelzer, P. Torrielli, and M. Zaro, The automated computation of tree-level and next-to-leading order differential cross sections, and their matching to parton shower simulations, *JHEP* **07**, 079, arXiv:1405.0301 [hep-ph].
- [27] F. Maltoni, D. Pagani, and I. Tsirikos, Associated production of a top-quark pair with vector bosons at NLO in QCD: impact on $t\bar{t}H$ searches at the LHC, *JHEP* **02**, 113, arXiv:1507.05640 [hep-ph].
- [28] R. Frederix, D. Pagani, and M. Zaro, Large NLO corrections in $t\bar{t}W^\pm$ and $t\bar{t}t\bar{t}$ hadroproduction from supposedly subleading EW contributions, *JHEP* **02**, 031, arXiv:1711.02116 [hep-ph].
- [29] T. Ježo and M. Kraus, Hadroproduction of four top quarks in the powheg box, *Phys. Rev. D* **105**, 114024 (2022), arXiv:2110.15159 [hep-ph].
- [30] N. Kidonakis and G. F. Sterman, Resummation for QCD hard scattering, *Nucl. Phys. B* **505**, 321 (1997), arXiv:hep-ph/9705234.
- [31] H. Contopanagos, E. Laenen, and G. F. Sterman, Sudakov factorization and resummation, *Nucl. Phys. B* **484**, 303 (1997), arXiv:hep-ph/9604313.
- [32] R. Bonciani, S. Catani, M. L. Mangano, and P. Nason, NLL resummation of the heavy quark hadroproduction cross-section, *Nucl. Phys. B* **529**, 424 (1998), [Erratum:

- Nucl.Phys.B 803, 234 (2008)], arXiv:hep-ph/9801375.
- [33] N. Kidonakis, E. Laenen, S. Moch, and R. Vogt, Sudakov resummation and finite order expansions of heavy quark hadroproduction cross-sections, Phys. Rev. D **64**, 114001 (2001), arXiv:hep-ph/0105041.
- [34] M. Czakon, A. Mitov, and G. F. Sterman, Threshold Resummation for Top-Pair Hadroproduction to Next-to-Next-to-Leading Log, Phys. Rev. D **80**, 074017 (2009), arXiv:0907.1790 [hep-ph].
- [35] M. Beneke, P. Falgari, and C. Schwinn, Soft radiation in heavy-particle pair production: All-order colour structure and two-loop anomalous dimension, Nucl. Phys. B **828**, 69 (2010), arXiv:0907.1443 [hep-ph].
- [36] V. Ahrens, A. Ferroglia, M. Neubert, B. D. Pecjak, and L. L. Yang, Renormalization-Group Improved Predictions for Top-Quark Pair Production at Hadron Colliders, JHEP **09**, 097, arXiv:1003.5827 [hep-ph].
- [37] M. Cacciari, M. Czakon, M. Mangano, A. Mitov, and P. Nason, Top-pair production at hadron colliders with next-to-next-to-leading logarithmic soft-gluon resummation, Phys. Lett. B **710**, 612 (2012), arXiv:1111.5869 [hep-ph].
- [38] M. Beneke, P. Falgari, S. Klein, and C. Schwinn, Hadronic top-quark pair production with NNLL threshold resummation, Nucl. Phys. B **855**, 695 (2012), arXiv:1109.1536 [hep-ph].
- [39] M. Czakon, A. Ferroglia, D. Heymes, A. Mitov, B. D. Pecjak, D. J. Scott, X. Wang, and L. L. Yang, Resummation for (boosted) top-quark pair production at NNLO+NNLL' in QCD, JHEP **05**, 149, arXiv:1803.07623 [hep-ph].
- [40] A. Kulesza, L. Motyka, T. Stebel, and V. Theeuwes, Soft gluon resummation for associated $t\bar{t}H$ production at the LHC, JHEP **03**, 065, arXiv:1509.02780 [hep-ph].
- [41] A. Kulesza, L. Motyka, T. Stebel, and V. Theeuwes, Soft gluon resummation at fixed invariant mass for associated $t\bar{t}H$ production at the LHC, PoS LHCP2016, 084 (2016), arXiv:1609.01619 [hep-ph].
- [42] A. Kulesza, L. Motyka, T. Stebel, and V. Theeuwes, Associated $t\bar{t}H$ production at the LHC: Theoretical predictions at NLO+NNLL accuracy, Phys. Rev. D **97**, 114007 (2018), arXiv:1704.03363 [hep-ph].
- [43] A. Kulesza, L. Motyka, D. Schwartländer, T. Stebel, and V. Theeuwes, Associated production of a top quark pair with a heavy electroweak gauge boson at NLO+NNLL accuracy, Eur. Phys. J. C **79**, 249 (2019), arXiv:1812.08622 [hep-ph].
- [44] A. Kulesza, L. Motyka, D. Schwartländer, T. Stebel, and V. Theeuwes, Associated top quark pair production with a heavy boson: differential cross sections at NLO+NNLL accuracy, Eur. Phys. J. C **80**, 428 (2020), arXiv:2001.03031 [hep-ph].
- [45] M. van Beekveld and W. Beenakker, The role of the threshold variable in soft-gluon resummation of the $t\bar{t}h$ production process, JHEP **05**, 196, arXiv:2012.09170 [hep-ph].
- [46] H. T. Li, C. S. Li, and S. A. Li, Renormalization group improved predictions for $t\bar{t}W^\pm$ production at hadron colliders, Phys. Rev. D **90**, 094009 (2014), arXiv:1409.1460 [hep-ph].
- [47] A. Broggio, A. Ferroglia, B. D. Pecjak, A. Signer, and L. L. Yang, Associated production of a top pair and a Higgs boson beyond NLO, JHEP **03**, 124, arXiv:1510.01914 [hep-ph].
- [48] A. Broggio, A. Ferroglia, G. Ossola, and B. D. Pecjak, Associated production of a top pair and a W boson at next-to-next-to-leading logarithmic accuracy, JHEP **09**, 089, arXiv:1607.05303 [hep-ph].
- [49] A. Broggio, A. Ferroglia, B. D. Pecjak, and L. L. Yang, NNLL resummation for the associated production of a top pair and a Higgs boson at the LHC, JHEP **02**, 126, arXiv:1611.00049 [hep-ph].
- [50] A. Broggio, A. Ferroglia, G. Ossola, B. D. Pecjak, and R. D. Sameshima, Associated production of a top pair and a Z boson at the LHC to NNLL accuracy, JHEP **04**, 105, arXiv:1702.00800 [hep-ph].
- [51] A. Broggio, A. Ferroglia, R. Frederix, D. Pagani, B. D. Pecjak, and I. Tsinikos, Top-quark pair hadroproduction in association with a heavy boson at NLO+NNLL including EW corrections, JHEP **08**, 039, arXiv:1907.04343 [hep-ph].
- [52] N. Kidonakis and A. Tonerio, Higher-order corrections in $t\bar{t}\gamma$ cross sections, (2022), arXiv:2212.00096 [hep-ph].
- [53] N. Kidonakis, G. Oderda, and G. F. Sterman, Threshold resummation for dijet cross-sections, Nucl. Phys. B **525**, 299 (1998), arXiv:hep-ph/9801268.
- [54] N. Kidonakis, G. Oderda, and G. F. Sterman, Evolution of color exchange in QCD hard scattering, Nucl. Phys. B **531**, 365 (1998), arXiv:hep-ph/9803241.
- [55] R. Bonciani, S. Catani, M. L. Mangano, and P. Nason, Sudakov resummation of multiparton QCD cross-sections, Phys. Lett. B **575**, 268 (2003), arXiv:hep-ph/0307035.
- [56] R. Frederix, S. Frixione, V. Hirschi, D. Pagani, H. S. Shao, and M. Zaro, The automation of next-to-leading order electroweak calculations, JHEP **07**, 185, [Erratum: JHEP 11, 085 (2021)], arXiv:1804.10017 [hep-ph].
- [57] V. Hirschi, R. Frederix, S. Frixione, M. V. Garzelli, F. Maltoni, and R. Pittau, Automation of one-loop QCD corrections, JHEP **05**, 044, arXiv:1103.0621 [hep-ph].
- [58] G. Ossola, C. G. Papadopoulos, and R. Pittau, CutTools: A Program implementing the OPP reduction method to compute one-loop amplitudes, JHEP **03**, 042, arXiv:0711.3596 [hep-ph].
- [59] F. Cascioli, P. Maierhofer, and S. Pozzorini, Scattering Amplitudes with Open Loops, Phys. Rev. Lett. **108**, 111601 (2012), arXiv:1111.5206 [hep-ph].
- [60] A. Denner, S. Dittmaier, and L. Hofer, Collier: a fortran-based Complex One-Loop Library in Extended Regularizations, Comput. Phys. Commun. **212**, 220 (2017), arXiv:1604.06792 [hep-ph].
- [61] S. Frixione, Z. Kunszt, and A. Signer, Three jet cross-sections to next-to-leading order, Nucl. Phys. B **467**, 399 (1996), arXiv:hep-ph/9512328.
- [62] S. Frixione, A General approach to jet cross-sections in QCD, Nucl. Phys. B **507**, 295 (1997), arXiv:hep-ph/9706545.
- [63] R. Frederix, S. Frixione, F. Maltoni, and T. Stelzer, Automation of next-to-leading order computations in QCD: The FKS subtraction, JHEP **10**, 003, arXiv:0908.4272 [hep-ph].
- [64] S. Catani and L. Trentadue, Resummation of the QCD perturbative series for hard processes, Nucl. Phys. B **327**, 323 (1989).
- [65] S. Catani, M. L. Mangano, and P. Nason, Sudakov resummation for prompt photon production in hadron collisions, JHEP **9807**, 024, hep-ph/9806484.

- [66] S. Catani, D. de Florian, M. Grazzini, and P. Nason, Soft gluon resummation for Higgs boson production at hadron colliders, *JHEP* **07**, 028, arXiv:hep-ph/0306211.
- [67] J. Botts and G. Sterman, Hard elastic scattering in qcd: Leading behavior, *Nuclear Physics B* **325**, 62 (1989).
- [68] N. Kidonakis and G. F. Sterman, Subleading logarithms in QCD hard scattering, *Phys. Lett. B* **387**, 867 (1996).
- [69] S. Keppeler and M. Sjö Dahl, Orthogonal multiplet bases in $SU(N_c)$ color space, *JHEP* **09**, 124, arXiv:1207.0609 [hep-ph].
- [70] M. van Beekveld, A. Kulesza, and L. Moreno Valero, in preparation.
- [71] S. Catani, M. L. Mangano, P. Nason, and L. Trentadue, The Resummation of soft gluons in hadronic collisions, *Nucl. Phys. B* **478**, 273 (1996), arXiv:hep-ph/9604351.
- [72] A. Manohar, P. Nason, G. P. Salam, and G. Zanderighi, How bright is the proton? A precise determination of the photon parton distribution function, *Phys. Rev. Lett.* **117**, 242002 (2016), arXiv:1607.04266 [hep-ph].
- [73] A. V. Manohar, P. Nason, G. P. Salam, and G. Zanderighi, The Photon Content of the Proton, *JHEP* **12**, 046, arXiv:1708.01256 [hep-ph].
- [74] J. Butterworth *et al.*, PDF4LHC recommendations for LHC Run II, *J. Phys. G* **43**, 023001 (2016), arXiv:1510.03865 [hep-ph].
- [75] R. D. Ball *et al.* (NNPDF), Parton distributions for the LHC Run II, *JHEP* **04**, 040, arXiv:1410.8849 [hep-ph].
- [76] L. A. Harland-Lang, A. D. Martin, P. Motylinski, and R. S. Thorne, Parton distributions in the LHC era: MMHT 2014 PDFs, *Eur. Phys. J. C* **75**, 204 (2015), arXiv:1412.3989 [hep-ph].
- [77] S. Dulat, T.-J. Hou, J. Gao, M. Guzzi, J. Huston, P. Nadolsky, J. Pumplin, C. Schmidt, D. Stump, and C. P. Yuan, New parton distribution functions from a global analysis of quantum chromodynamics, *Phys. Rev. D* **93**, 033006 (2016), arXiv:1506.07443 [hep-ph].